Materials Science Forum Vol. 767 (2014) pp 46-51
Online available since 2013/Jul/31 at www.scientific.net

doi:10.4028/www.scientific.net/MSF.767.46

Experimental and Numerical Study on the Afterburning Effect of TNT

Cao Wei[1, a], He Zhongqi[1,b] and Chen Wanghua[1,c]

[1] School of Chemical Engineering, Nanjing University of Science and Technology, 200 Xiaolingwei St., Nanjing 210094, Jiangsu, China

[a]weicao668@163.com, [b]hzq555@163.com, [c]chenwh_nust@163.com

Keywords: afterburning, TNT, open space, double-layer container, numerical simulation

Abstract. In order to investigate the afterburning effect of TNT in an open space, a double-layer container (DLC) which can be filled with different gases and enhance the afterburning effect of underoxidized explosives was designed. The charges were located in the inner container, and the outer container was filled with different gases (air, oxygen or nitrogen). The experiments were conducted under water. After initiation, the DLC cracks and provides gas for the detonation products. Underwater static pressure transducer was the main diagnostic. It is shown that pressure and impulse histories for explosions in oxygen and air are greater than those recorded for explosions in nitrogen. Moreover, the afterburning energy was calculated. Results show that the afterburning energy increases with the increase of the amount of oxygen, but cannot reach the theoretically maximum value even though there is excessive oxygen. Finally, two-dimensional numerical simulations were performed by the explicit finite element program ANSYS AUTODYN. The Miller energy release model was used to describe the afterburning process. Results demonstrate that computed pressure histories agreed with measured pressure histories well in terms of initial peak pressure, waveforms and total impulse.

Introduction

The products of detonation of an underoxidized explosive are themselves fuels. These are normally products such as CO and free carbon. When these expand and mix with air, they eventually reach the lower combustion limit for these materials, and if they are at high enough temperature, or there is some other ignition source present, they will burst into flame [1]. For this reason, the combustion that takes place after the detonation reaction zone is called afterburn. This afterburn can be very energetic, cause a slow decay of shock wave and increase the lethality of ammunition.

Such combustion effect was first studied by Ornellas [2] in a 5.28 dm^3 calorimetric bomb. He measured the heat of 25 g TNT detonated in vacuum and oxygen respectively. Results show that the heat measured in vacuum is 4573±46 $J \cdot g^{-1}$, which is in good agreement with the detonation heat (4740±63 $J \cdot g^{-1}$) predicted by thermodynamic equilibrium code CHEETAH [3]. The heat measured in 246 kPa oxygen is 14958±146 $J \cdot g^{-1}$, which is close to the combustion heat (15037±251 $J \cdot g^{-1}$) predicted by CHEETAH. In addition, Kiciński et al. [4] measured the heats of explosion of non-ideal RDX-based compositions in a calorimetric bomb of 5.6 dm^3 under high pressure of four various atmospheres (argon, nitrogen, air and argon/oxygen). It is shown that the presence of oxygen in the compressed gas filling a bomb leads to complete combustion of the detonation products and aluminum particles, explosion heats of all tested mixtures are almost the same in argon and nitrogen atmosphere.

The afterburning effect of the detonation products of condensed explosive in steel chambers was also studied in the past couple of years [5-7], the chambers were filled with different gases (air, oxygen and nitrogen et al.) and the pressure histories in the chambers were measured and analyzed. Kuhl et al. [8] also gave a model to simulate the turbulent combustion in confined TNT explosions, the predicted pressures histories are quite similar to the measured pressures histories for all cases studied.

However, the above experiments were conducted in a confined space. In this work, the experiments were conducted in an open space under water. We used a double layer container (DLC), comprising an inner container containing charge assembly, and an outer container surrounding the inner container and containing high pressure gas to enhance the afterburning effect. Both the shock wave histories and afterburning energy were obtained from the underwater explosion experiments. A comprehensive description of the sequence of events that take place in an underwater explosion and the scientific principles needed to analyze such events can be found in the account by Cole [9]. Underwater firing of explosives provides a valuable means of assessing the performance under conditions which are safe and reproducible, realistically large charges can be fired and the effects transmitted to the water are easily measured for example with a pressure transducer [10]. Two-dimensional numerical simulations were also performed by the explicit finite element program ANSYS AUTODYN [11]. JWL equation of state (EOS) with Miller energy release model extension [12] was used in the numerical modeling. Computed pressure histories were compared with measured pressure histories.

Experimental Section

The charge assembly consisted of a 200 g TNT ($C_7H_5N_3O_6$, oxygen balance=－0.74, detonation heat Q_v=4.5 kJ·g^{-1}) charge, a 5 g cylindrical pressed JH-14 (96.5% RDX and 3.5% fluororubber and graphite in mass, 1.72 g·cm^{-3} in density, 15 mm in diameter) booster, and a no.8 electric detonator. The TNT was pressed to a density of 1.58 g·cm^{-3}, in the form of cylindrical plug (4 cm in diameter).

In order to enhance the afterburning effect of underoxidized explosive, a DLC filled with different gases was used. The dimensional sketch of DLC is presented in Fig. 1. The outer container of a volume of 6.024 L was filled with different gases through a valve , the charge assembly was put at the bottom of the inner container, and finally the DLC was made waterproof and put into water. The gases used in this research were oxygen, air and nitrogen under pressure of 4.6 and 0.6 MPa (absolute pressure, similarly hereinafter). The material of DLC is alloy steel C20E4 (ISO 683/18), the toroidal parts are made of seamless pipes and welded to the both endplates. After initiation, the DLC cracks and provides gas for the detonation products. When these products are mixed with air or oxygen, it forms a turbulent combustion and liberates additional energy.

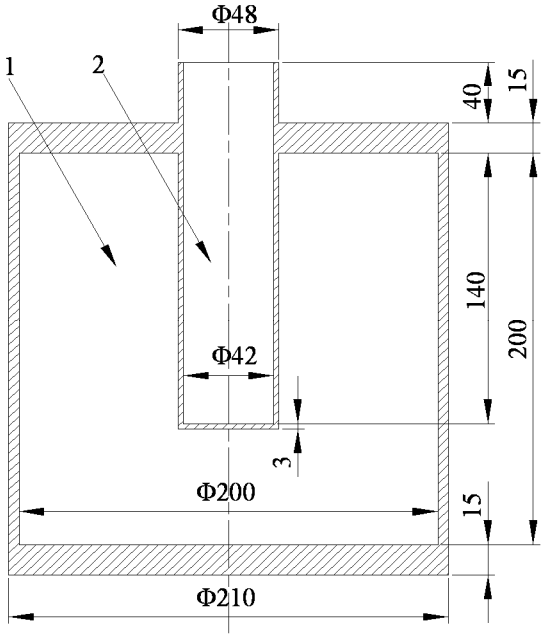

Figure 1. Dimensional sketch of the DLC: 1 – outer container; 2 – inner container (Unit: mm).

The pressure histories were collected and recorded by an internal circuit piezoelectric crystal pressure transducer (PCB 138M124), a sensor signal conditioner (PCB 482A16), and a data collecting instrument (JOVIAN 5200).The experiments were conducted in a Φ8 m×8 m rigid pool. At least two tests were performed for each atmosphere investigated. Fig. 2 shows the scheme of experimental disposal. The explosion centre and the pressure transducer were at the same level as the horizon, and 4.25 m below the surface of water. The distance between explosion centre and pressure transducer was 2.5 m.

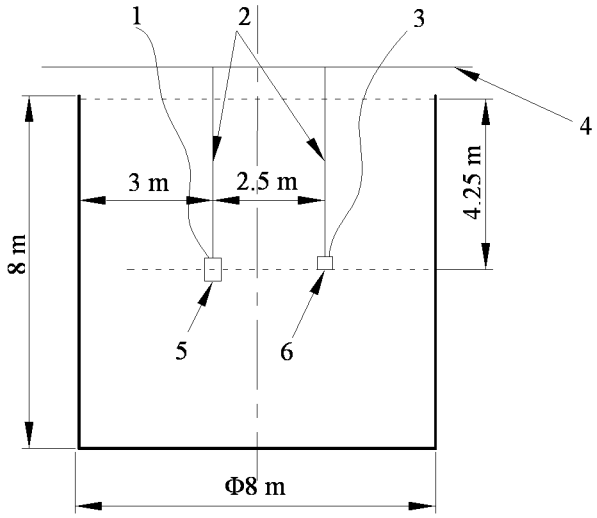

Figure 2. Scheme of experimental disposal: 1 – ignition cable; 2 – load rope; 3 – transmission cable; 4 – experimental holder; 5 – DLC; 6 – pressure transducer.

Experimental Results and Discussion

Shock Wave Histories

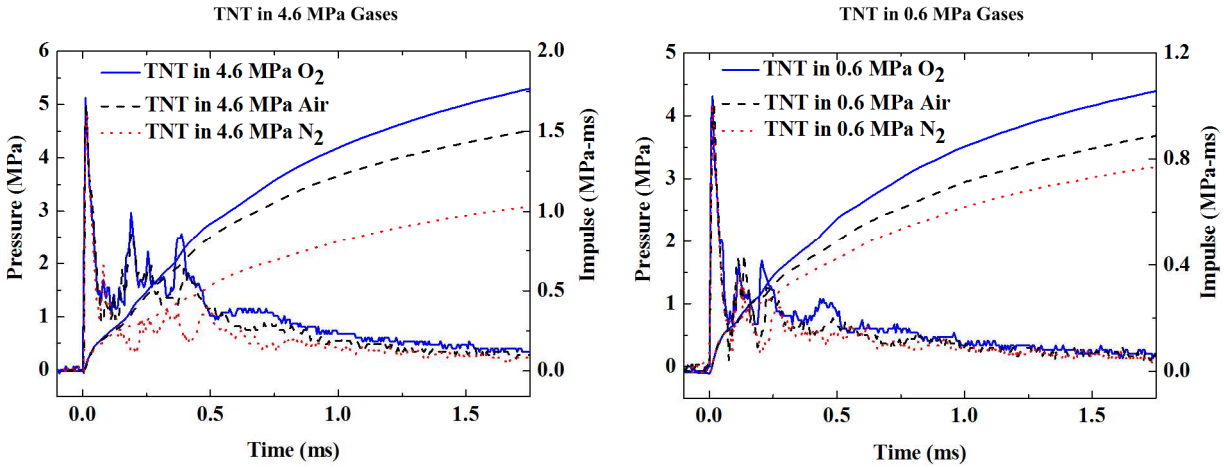

Figure 3. Comparison of pressure and impulse histories of TNT measured in 4.6 and 0.6 MPa gases.

Fig. 3 presents comparisons of pressure and impulse histories of TNT measured in 4.6 and 0.6 MPa gases. Solid curves represent results from explosion in oxygen, dash curves denote results from explosion in air and dot curves correspond to results from explosion in nitrogen. Pressure and impulse histories for explosions in oxygen and air are greater than those recorded for explosions in nitrogen. Pressure enhancement (i.e., the solid and dash curves versus the dot curves) is a consequence of combustion of the explosion production gases with oxygen or air. Here nitrogen is used as inert gas

[4]. This combustion effect (i.e. afterburning effect) is enhanced with the increase of the amount of oxygen. For example, the afterburning effect is weakest in 0.6 MPa air, but most pronounced in 4.6 MPa oxygen.

Afterburning Energy

The values of specific shock wave energy e_s, specific bubble energy e_b and specific total energy e_t were calculated by the method described by Bjarnholt [10]. Results are given in Table 1. Considering that the shock wave pressure decays slowly to the baseline, the shock wave energy is integrated to time 51.7θ in this paper instead of 6.7θ in Ref. [10] (the time constant θ is defined as the time it takes for the pressure to decay from its first peak value p_m to a value p_m/e i.e. $0.37p_m$).

The values in Table 1 are the average of two parallel tests results. It can be seen in Table 1, that the values of e_s, e_b and e_t under pressure 4.6 MPa have a visible increase versus those under pressure 0.6 MPa for the same gas (oxygen, air or nitrogen). The increase in specific shock wave energy and specific bubble energy not only results from the stronger afterburning effect under pressure 4.6 MPa (for oxygen and air), but also from the inherent higher pressure gases under pressure 4.6 MPa (for oxygen, air and nitrogen).

Table 1. Underwater explosion energy of TNT under varying conditions of gases.

Gaseous filler	e_s [kJ·g^{-1}]	e_b [kJ·g^{-1}]	e_t [kJ·g^{-1}]	e_t/Q_v [%]
0.6 MPa N_2	0.21	1.81	2.17	48.2
0.6 MPa air	0.22	2.24	2.66	59.1
0.6 MPa O_2	0.30	3.27	3.89	86.4
4.6 MPa N_2	0.28	3.32	3.87	86.0
4.6 MPa air	0.56	5.09	6.30	140.0
4.6 MPa O_2	0.68	7.23	8.77	194.6

It has been proved in Ref. [4] that nitrogen doesn't take part in the afterburning reaction of underoxidized explosive, so the afterburning energy can be calculated by subtracting the total energy released in nitrogen from the total energy released in oxygen or air under the same pressure. The calculated specific afterburning energy e_a is shown in Table 2. The values in Table 2 are in good accordance with the pressure and impulse histories in Fig. 3, and the specific afterburning energy reaches the maximum value of 108.9 % of the detonation heat.

Table 2. Specific afterburning energy of TNT under varying conditions of gases.

Gaseous filler	e_a [kJ·g^{-1}]	e_a/Q_v [%]
0.6 MPa air	0.49	10.9
0.6 MPa O_2	1.72	38.2
4.6 MPa air	2.43	54.0
4.6 MPa O_2	4.90	108.9

Theoretically, the maximum energy released by afterburning reaction of TNT is about 10.4 kJ·g^{-1} [1,2]. There is excessive oxygen in 4.6 MPa oxygen to burn all the reduction elements in TNT (without consideration of cab and booster) to their most highly oxidized products, but as shown in Table 2 that the afterburning energy released in 4.6 MPa oxygen (4.90 kJ·g^{-1}) doesn't reach the theoretical maximum value (10.4 kJ·g^{-1}). It is inferred that detonation products are not fully consumed. The probable reason is that the temperature and pressure inside the bubble quickly fall to a level at which the afterburning reaction is quenched. This result of an open space is different from that of confined explosion, where the presence of excessive oxygen in the compressed gas filling a bomb leads to complete combustion of the detonation products [2,4].

Numerical Simulation

Numerical Modeling

Numerical simulation was based on the explicit finite element program ANSYS AUTODYN. All material models were chosen from AUTODYN. The standard JWL model [13] takes no account of the afterburning energy. In order to model the time dependent afterburning energy release, the standard JWL EOS was extended using the approach proposed by Miller [12]. The JWL EOS with Miller extension used for the explosive part is as follows

$$p = A\left(1-\frac{\omega}{R_1 V}\right)\exp(-R_1 V)+B\left(1-\frac{\omega}{R_2 V}\right)\exp(-R_2 V)+\frac{\omega E+\lambda Q}{V}, \tag{1}$$

where p is pressure, V is relative volume, T is temperature, A, B, R_1, R_2 and ω are constants, E is the energy content of the explosive that sustains the detonation CJ conditions, Q is the afterburning energy release after the CJ plane, and λ is the fraction of reacted detonation products and is given by

$$\frac{\mathrm{d}\lambda}{\mathrm{d}t} = a(1-\lambda)^m p^n, \tag{2}$$

where a is afterburning coefficent, m is energy release exponent and n is pressure exponent.

Numerical Results and Analysis

Pressure and impulse histories of TNT in 4.6 and 0.6 MPa oxygen from numerical simulation of the 2-d combustion field are presented in Fig. 4. The computed pressure and impulse histories of spot 2.5 m from the explosion centre were compared with those measured in experiments. Reuslts show that the computations agree nicely with the experimental data—judged on the basis of initial peak pressure, waveforms and total impulse.

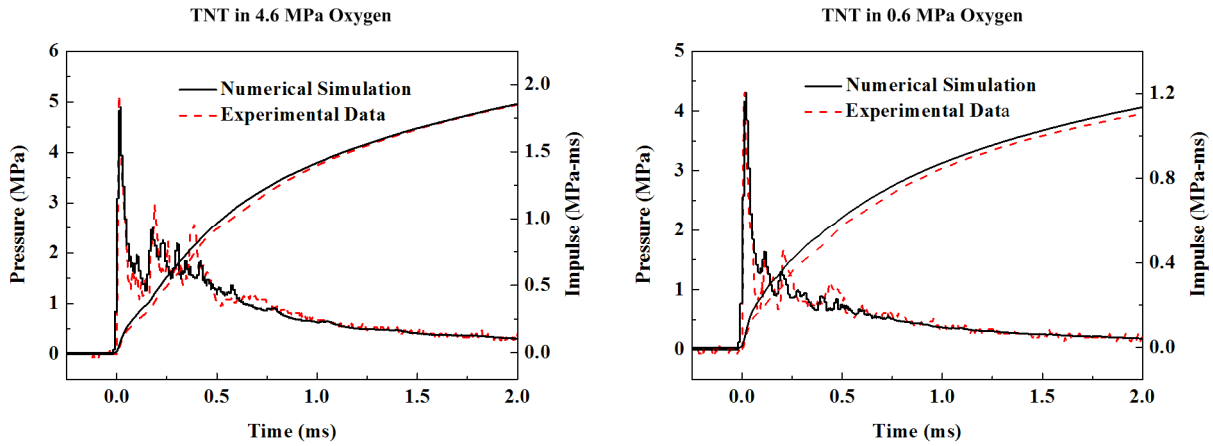

Figure 4. Comparison of pressure and impulse histories from numerical simulation with experimental data.

Conclusion

In this paper, we have attempted several things. First, we have shown the pressure and impulse enhancements in an open space due to afterburning reaction in oxygen and air. The gas is provided by a DLC, which is designed to enhance the afterburning effect of underoxidized explosive. Secondly, we have calculated the afterburning energy by underwater explosion tests. Results show that the afterburning energy increases with the increase of the amount of oxygen, but cannot reach the theoretically maximum value even though there is excessive oxygen. These results mean that the afterburning energy released in an open space is different from that in confined explosion, where the presence of excessive oxygen in the compressed gas filling a bomb leads to complete combustion of

the detonation products. Thirdly, we have simulated the afterburning reaction by using JWL EOS with Miller extension. Computed pressure histories agree with measured pressure histories well for all cases studied.

Acknowledgements

This research was supported by the Basic Products Innovation Project of Defense Industrial Technology Development Program of China. We wish to thank Prof. Liu Ronghai, Prof. Peng Jinhua and Dr. Rao Guoning et. al. for their valuable advice and assistant in carrying out this work.

References

[1] P.W. Cooper, Explosives Engineering, VCH Publishers, New York, 1996.

[2] D.L. Ornellas, Calorimetric Determinations of the heat and products of detonation of explosives, Report UCRL-52821, Lawrence Livermore National Laboratory, Livermore, CA, USA, 1982.

[3] L.E. Fried, CHEETAH 1.22 user's manual, Report UCRL-MA-117541, Lawrence Livermore National Laboratory, Livermore, CA, USA, 1995.

[4] W. Kiciński, W.A. Trzciński, Calorimetry studies of explosion heat of non-ideal explosives, J. Therm. Anal. Calorim. 96 (2009) 623-630.

[5] P. Wolański, Z. Gut, W.A. Trzciński, L. Szymańczyk, J. Paszula, Visualization of turbulent combustion of TNT detonation products in a steel vessel, Shock Waves 10 (2000) 127-136.

[6] W. A. Trzciński, S. Cudziło, J. Paszula, Studies of free field and confined explosions of aluminium enriched RDX compositions, Propellants, Explos., Pyrotech. 32 (2007) 502-508.

[7] A.L. Kuhl, H. Reichenbach, Combustion effects in confined explosions, Proc. Combustion Inst. 32, (2009) 2291-2298.

[8] A.L. Kuhl, J.B. Bell, V.E. Beckner, H. Reichenbach, Gasdynamic model of turbulent combustion in TNT explosions, Proc. Combustion Inst. 33 (2011) 2177-2185.

[9] R.H. Cole, Underwater Explosions, Princeton University Press, Princeton, 1948.

[10] G. Bjarnholt, Suggestions on standards for measurement and data evaluation in the underwater explosion test, Propellants, Explos., Pyrotech. 5 (1980) 67-74.

[11] ANSYS Inc., AUTODYN User Manual Version 11.0, 2007.

[12] P.J. Miller, A reactive flow model with coupled reaction kinetics for detonation and combustion in non-ideal explosives, Mat. Res. Soc. Symp. Proc. 418 (1996) 413-420.

[13] E.L. Lee, H.C. Horning, J.W. Kury, Adiabatic expansion of high explosive detonation products, Report UCRL-50422, Lawrence Radiation Laboratory, Livermore, CA, USA, 1968.

Explosion, Shock Wave and High-Energy Reaction Phenomena II
10.4028/www.scientific.net/MSF.767

Experimental and Numerical Study on the Afterburning Effect of TNT
10.4028/www.scientific.net/MSF.767.46

DOI References
[4] W. Kiciński, W.A. Trzciński, Calorimetry studies of explosion heat of non-ideal explosives, J. Therm. Anal. Calorim. 96 (2009) 623-630.
http://dx.doi.org/10.1007/s10973-008-9100-5
[5] P. Wolański, Z. Gut, W.A. Trzciński, L. Szymańczyk, J. Paszula, Visualization of turbulent combustion of TNT detonation products in a steel vessel, Shock Waves 10 (2000) 127-136.
http://dx.doi.org/10.1007/s001930050186
[6] W. A. Trzciński, S. Cudziło, J. Paszula, Studies of free field and confined explosions of aluminium enriched RDX compositions, Propellants, Explos., Pyrotech. 32 (2007) 502-508.
http://dx.doi.org/10.1002/prep.200700202
[8] A.L. Kuhl, J.B. Bell, V.E. Beckner, H. Reichenbach, Gasdynamic model of turbulent combustion in TNT explosions, Proc. Combustion Inst. 33 (2011) 2177-2185.
http://dx.doi.org/10.1016/j.proci.2010.07.085
[10] G. Bjarnholt, Suggestions on standards for measurement and data evaluation in the underwater explosion test, Propellants, Explos., Pyrotech. 5 (1980) 67-74.
http://dx.doi.org/10.1002/prep.19800050213
[12] P.J. Miller, A reactive flow model with coupled reaction kinetics for detonation and combustion in non-ideal explosives, Mat. Res. Soc. Symp. Proc. 418 (1996) 413-420.
http://dx.doi.org/10.1557/PROC-418-413